Proceedings of Insert Conference Abbreviation
Insert Conference Name
Insert Conference Date and Location

Paper Number Here

Material Modeling for Shape Deposition Manufacturing of Biomimetic Components

Xiaorong Xu[1], Wendy Cheng[1], Daniel Dudek[2], Motohide Hatanaka[1], Mark R. Cutkosky[1], and Robert J. Full[2]

[1]Stanford University, Center for Design Research; Stanford, CA 94305, xiaorong@cdr.stanford.edu
[2]University of California at Berkeley, Dept. of Integrative Biology; Berkeley, CA 94720

ABSTRACT

As our understanding of the principles underlying animal locomotion improves, we are inspired to apply them to robot design. This has traditionally been achieved through controls or discrete mechanical devices; however, new manufacturing methods, such as Shape Deposition Manufacturing (SDM), offer us the opportunity to develop mechanisms containing intrinsic mechanical properties tailored for function. To properly utilize SDM, we must develop a bridge between biology and design. As a first step, we have conducted relaxation and dynamic tests on the ablated metathoracic limb of the *Blaberus discoidalis* cockroach and derived measures of stiffness and damping. We then tested an SDM-compatible polymer with similar viscoelastic properties. Comparison and understanding of the mapping between these two materials enables us to design and manufacture legs with stiffness and damping similar to those found in insects.

NOMENCLATURE

B	geometric constant associated with relaxation analysis
C	damping constant
E	modulus of elasticity
G	shear modulus
I	moment of inertia
K_{leg}	stiffness of a leg
K_{rel}	stiffness normalized by weight
L_{joint}	moment arm for torsion
L	characteristic length
M	moment
l	moment arm
m	mass
Δ	phase shift between force and displacement
θ	angular displacement in time domain
τ	time constant equal to μ / E_1
$(\ )_0$	amplitude or initial value
$(\ )_1$	transient part of modulus/stiffness
$(\ )_2$	storage part of modulus/stiffness
$(\ )_r$	quantity associated with relaxation experiments
$(\ )'$	dynamic storage modulus
$(\ )''$	dynamic loss modulus
$(\ )^*$	complex conjugate

INTRODUCTION

Materials found in Nature differ significantly from those found in human-made devices. Nature appears to design for “bending without breaking” and employs tissues that are compliant and viscoelastic [Vogel, 1995] rather than stiff, homogenous, and isotropic. Even “stiff” natural materials, such as the calcified shells of crabs, have local areas that bend, buckle and bulge during motion [Blickhan, Full, and Ting, 1993]. In addition, local variations in biological materials, tailored to meet local variations in loading, are common.

The nonlinear, compliant, and inhomogenous materials found in even the simplest animals provide them with a sophistication and robustness that today's robots cannot match. However, as our ability to analyze and fabricate mechanisms with compliant and functionally-graded materials improves, we have the opportunity to develop robots whose structures draw inspiration

from simple animals such as insects and crustaceans.

One fertile area for biomimetic design is the legs of walking or hopping robots, where leg compliance has been recognized as especially important [Raibert, 1986]. Biologists studying subjects ranging from mammals to arthropods have also shown that natural legs are carefully designed and tuned for passive compliance. The deathhead cockroach (*Blaberus discoidalis*) possesses legs with compliant muscles and skeletal components that increase dynamic stability and disturbance rejection [Full and Koditschek, 1999] [Kubow and Full, 1999] [Meijer and Full, in press]. Leg compliance also varies dynamically. Running animals adjust the overall compliance of their legs to decrease impact forces and minimize energy costs [Alexander, 1990] while humans adjust their leg compliance to accommodate changes in surface hardness, stride frequency, mass, and leg inertia [Ferris, et al, 1998] [Farley, et al, 1998] [Farley and Gonzalez, 1996] [Obusek, et al, 1995].

For mobile robots to approach the speed and robustness of legged animals, we are inspired to reproduce some of the critical mechanical parameters found in natural legs. These characteristics - such as compliance - have traditionally been achieved through either sensing and control algorithms or discrete mechanical devices such as coil springs and pneumatic cylinders. However, inherent advantages exist in producing these parameters through mechanisms with intrinsic properties and local variations tailored for locomotion; with this approach, we can simplify controls and fabricate robots possessing robustness and speed closer to those of simple animals.

One method for manufacturing such robots is Shape Deposition Manufacturing (SDM), a rapid prototyping technology [Merz *et al.*, 1994]. SDM addresses many of the limitations of traditional manufacturing and assembly methods by enabling the simultaneous fabrication and assembly of mechanisms with complex geometry and heterogeneous materials [Binnard, 1999] [Cham et al, 1999] [Bailey et al, 1999].

Design and fabrication of layered and heterogeneous materials (also called Functionally Graded Materials - FGMs) has recently been a focus of research [Fessler et al, 1997]. For the manufacture of biomimetic components, FGMs enable us to control local variations by selectively depositing soft and hard materials.

To produce biologically inspired components of biomimetic mechanical properties, a bridge between biological findings and SDM design specifications is needed. The first requirement is to characterize biological structures and translate the characteristics into quantitative specifications for mobile robots. The second requirement is to model SDM material behavior to facilitate component design to meet these specifications.

To address these requirements we first performed experiments on a hind leg of *Blaberus discoidalis* and described its response to both step displacement inputs and sinusoidal displacement excitations. Next, we tested one of the materials used in SDM, a polyurethane polymer chosen for its qualitative similarity to insect cuticle, and fit the results to standard viscoelastic materials and models. Comparison and understanding of the mapping between these two studies enable us to begin to design and manufacture legs similar to those found in biology.

BIOLOGICAL CHARACTERIZATION

The cockroach legs and urethane polymers are both composed of long molecular chains. These chains move with respect to each other during macroscopic deformation, causing the material to exhibit viscoelastic behavior such as stress relaxation, creep, unrecoverable deformation, and hysteresis.

To obtain specific viscoelastic measures of standard materials, creep, relaxation, or dynamic experiments are performed and the results fit to the Maxwell, Voigt, or Standard Linear Solid models (Fig. 1). Researchers have also used these models to fit biological materials such as human bones and rabbit skin [Lakes, 1979] [Fung, 1994].

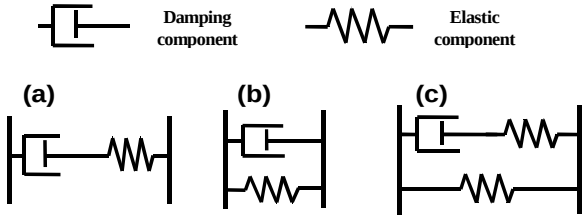

Figure 1. Viscoelastic models. (a) Maxwell model, (b) Voigt model, and (c) standard linear model.

Experiment Setup and Results

Relaxation and dynamic experiments were carried out on the hind leg of *Blaberus discoidalis* to aid in the selection of a material behavior model and to quantify measures of roach leg response. During testing, the coxa of the ablated metathoracic limb (hind limb) of the cockroach was epoxied to 3/8” plexi-glass such that the coxa-femur and femur-tibia joints were free to rotate. One end of a stainless steel pin was attached to the distal tip of the tibia with cyanoacrylate and the other end to the arm of a servo-motor system (Aurora Scientific, Inc.) with dental impression compound (Kerr). The servo-motor system inputs a time variant deflection while simultaneously measuring force (Fig. 2). The error associated with the entire system is estimated to be less than 4 %.

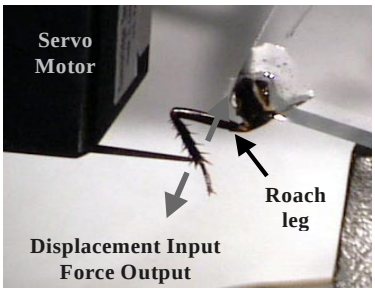

Figure 2. Cockroach hind leg test setup.

The cockroach leg was displaced in a direction orthogonal to the joint motion at amplitudes of 0.1 mm, 0.3 mm, 0.5 mm, 0.7 mm, and 1.0 mm. These values were chosen since observations of locomoting *Blaberus* show that the deflection of the hind leg in this direction was less than 1.0 mm. Step inputs at these amplitudes produced relaxation histories where the reaction forces initially peaked and then attenuated to constant force levels (Fig. 3).

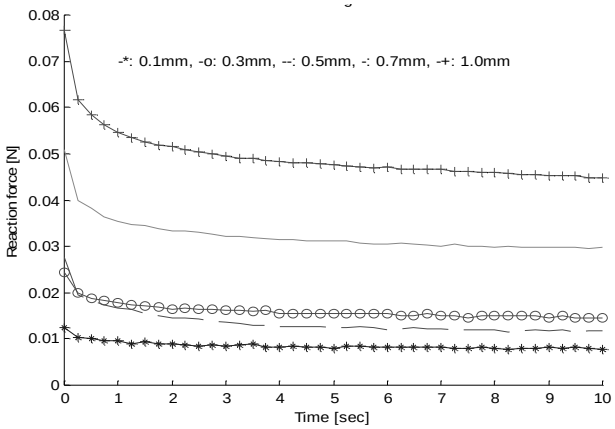

Figure 3. Reaction force relaxation histories of the *Blaberus* leg in response to step displacement inputs at five amplitudes.

Dynamic tests with sinusoidal displacement inputs ranging in frequency from 0.01 Hz to 100 Hz were performed. The *Blaberus* has a preferred trotting frequency of approximately 12 Hz, at which it behaves similar to an inverted spring/pendulum [Full and Tu, 1990] [Blickhan and Full, 1993]. At low frequencies and small amplitudes, the force-displacement hysteresis curve was very similar to that expected for a linear viscoelastic solid (Fig. 4a). As the frequency and amplitude increased, the response grew increasingly nonlinear such that, at vibration frequency greater than 40 Hz, the curve became skewed (Fig. 4b). Therefore, some of the data such as phase angle are calculated only for frequencies equal to or lower than 40 Hz. In addition, some of the force-displacement plots are not centered about zero-zero due to an initial negative force offset present during the trials.

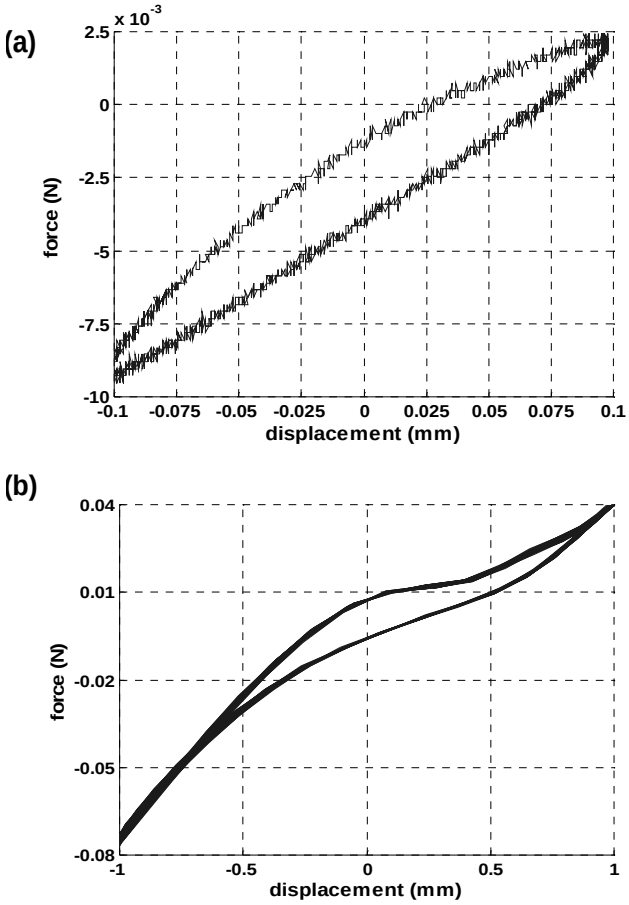

Figure 4. Force-displacement response for the *Blaberus* leg under sinusoidal deflections. (a) 0.02 Hz and 0.01 mm, (b) 50 Hz and 1.0 mm.

Associated with this hysteresis curve is a phase shift in which the measured output force leads the input displacement. This phase shift is similar to the 'loss angle' in viscoelastic materials. Fig. 5 plots the phase shift for vibration frequencies between 0.01 Hz and 50 Hz, where the hysteresis curve approximates that of a viscoelastic solid. At low frequencies, an average stiffness of 45 N/m can be directly read from the plots by taking the slope of the line connecting the tips of the force-displacement loops [Blickhan, 1986].

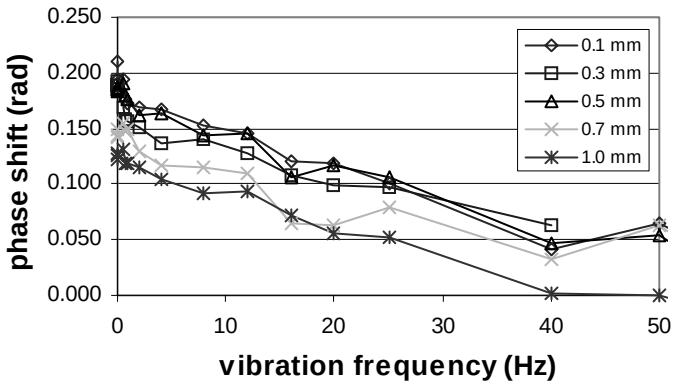

Figure 5. Phase shift (force leads displacement) from sinusoidal displacement inputs.

Model of cockroach leg

The results of these tests indicate that a cockroach leg excited in a direction orthogonal to the joint direction behaves similarly to a viscoelastic material. The exponential nature of the force relaxation curves suggests viscoelasticity. The hysteretic nature of the force-displacement curves indicates that there is energy loss due to the internal friction, which is a common characteristic for viscoelastic materials.

The cockroach leg and joints are subject to a combination of bending and torsion in the experiment. The overall effect can be modeled as a torsion spring with a moment arm (Fig. 6). Additional assumptions for the model include:

1. The axis of rotation for the leg is kept approximately constant during torsion.
2. The joint material can be approximated using a lumped-parameter element with uniformly distributed linear viscoelastic properties.

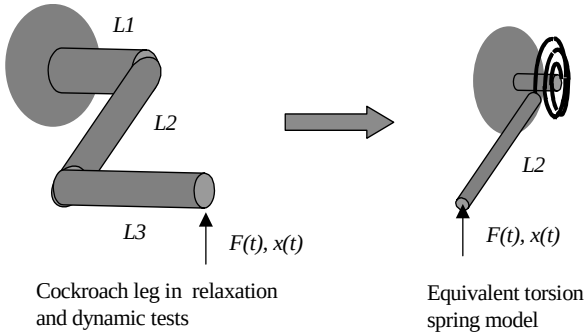

Figure 6. Model of the cockroach leg as a torsion spring with a moment arm.

Model of relaxation test results. With this simplification, the relaxation test results imply that the step response of a cockroach leg under a constant rotation angle can be mathematically described by:

$$M_r(t) = B\theta_0(G_2 + G_1 e^{-t/\tau_r}) \qquad \text{(Eq. 1)}$$

Where $M_r(t)$ is the reaction moment relaxation history due to the step angular input θ_0, B is a constant associated with the leg and joint geometry, G_1 is the transient part of the shear modulus, and G_2 is the equilibrium shear modulus after infinite time.

Recognizing that torsion is caused by the force applied on the tip of the tibia, one can rewrite Eq. 1 as a relation between force and displacement:

$$f_r(t) = \frac{Ba_0}{l^2}(G_2 + G_1 e^{-t/\tau_r}) \qquad \text{(Eq. 2)}$$

Where $f_r(t)$ is the reaction force recorded in the relaxation experiment, a_0 is the amplitude of the sinusoid deflection, and l is the arm of the torque moment.

Eq. 2 can be solved for BG_1 and BG_2 by considering the cases of $t = 0$ and as t approaches infinity:

$$BG_1 = \frac{l^2}{a_0}[f(0) - f(\infty)] \text{ and } BG_2 = \frac{l^2}{a_0}f(\infty). \qquad \text{(Eq. 3)}$$

By plugging the force-displacement relation (Eq. 2) into the cockroach leg relaxation data (Fig. 3), one can obtain the time constant τ_r as 1.92 seconds. The exponential expression of the shear modulus is not available since the geometric factor B is unknown. However, we can derive that $BG_1 = 3.67 \times 10^{-3}(Nm)$ and $BG_2 = 3.2 \times 10^{-3}(Nm)$.

Correlation with Standard Linear Model. The experiments on the cockroach leg can be modelled from a linear perspective as shown in Fig. 7. The force and displacement relation in the frequency domain for this system is:

$$\frac{F(s)}{X(s)} = \frac{C(K_1 + K_2)s + K_1K_2}{Cs + K_1}. \qquad \text{(Eq. 4)}$$

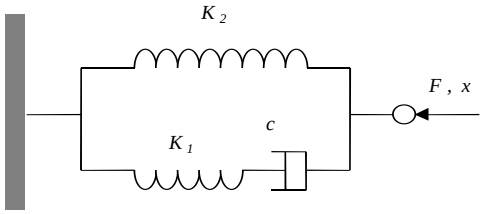

Figure 7. Macroscopic model of cockroach leg used for analysis of displacement step response.

By comparing the step response predicted by this model with

Eq. 2, one can obtain simple expressions of the stiffness and damping parameters from the viscoelastic property data.

$$K_1 = \frac{BG_1}{l^2},\ K_2 = \frac{BG_2}{l^2},\ \text{and}\ c = \frac{BG_1}{l^2}\tau_r \qquad \text{(Eq. 5)}$$

For the cockroach leg, K_1 = 34.5 N/m, K_2 = 29.8 N/m and C = 49.4 Ns/m.With K_1, K_2 and C, one can predict the force relaxation history as shown in figure 8. Figures 3 and 8 are then compared for evaluation of the modeling accuracy and possible experiment errors.

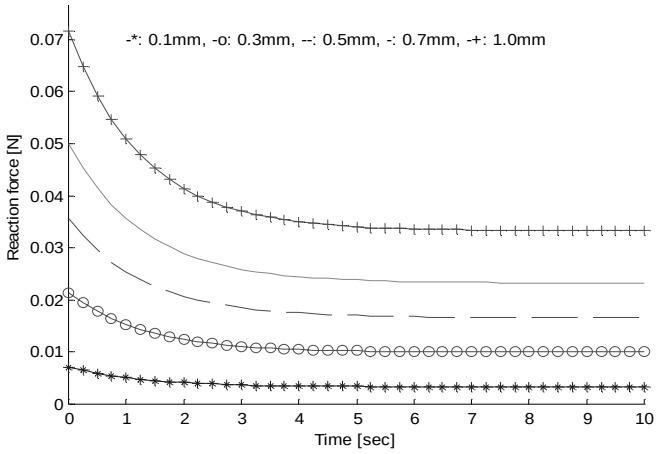

Figure 8. Relaxation force history predicted by spring-damper model.

Model of sinusoidal excitation test results. The torsion spring representation of the cockroach leg can also be applied to analyze the dynamic response of the leg. The force response is due to a combination of the reaction moment of the material and the moment associated with the inertia of the leg and the stainless steel pin.

$$M_e = G^* k\theta + I\frac{d^2\theta}{dt^2} \qquad \text{(Eq. 6)}$$

Where G^* is the complex form of the dynamic modulus combining G', the dynamic storage modulus, and G'', the dynamic loss modulus.

$$G^* = G' + G''i \qquad \text{(Eq. 7)}$$

The sinusoid angular input in complex form is:

$$\theta = \theta_0 e^{i\omega t} \qquad \text{(Eq. 8)}$$

The dynamic response of the cockroach leg in the complex form is therefore:

$$f(t) = \frac{a_0}{l^2} e^{i\omega t}[(BG' - I\omega^2) + BG''i] \qquad \text{(Eq. 9)}$$

Where ω is the angular velocity of the vibration and a_0 is the amplitude of the vibration.

Similar to the force relaxation case, results from the dynamic experiment can not yield exact expressions of material shear moduli, but rather with a geometric factor B:

$$BG' = I\omega^2 + \frac{F_0 l^2}{a_0\sqrt{1+(\tan\Delta)^2}},\ \text{and}\ BG'' = \frac{F_0 l^2 \tan\Delta}{a_0\sqrt{1+(\tan\Delta)^2}} \qquad \text{(Eq. 10)}$$

Where Δ is the phase shift (loss angle) of the force versus the displacement, F_0 is the amplitude of the force (i.e., applied force minus inertia force), and l is the length of the moment arm for the input force. Application of the above expressions to the dynamic test data yields the dynamic storage and loss moduli (multiplied by the geometric factor) as functions of the vibration frequency and amplitude.

Correlation with Voigt model. The simpliest linear model can be used to fit the dynamic response data is the Voigt model. Experimental results show that the input displacement (x) and the output force (f) differ mainly in magnitude and a phase shift (Δ). Mathematically, they can be described by:

$$x(t) = X_0\cos(\omega t)\ \text{and}\ f(t) = F_0\cos(\omega t + \Delta). \qquad \text{(Eq. 11)}$$

Taking the Laplace transform of Eq. 11 and solving for the transfer function *F(s)/X(s)* yields:

$$\frac{F(s)}{X(s)} = \frac{F_0}{X_0}\left(\frac{\sin(\Delta)}{\omega}s + \cos(\Delta)\right). \qquad \text{(Eq. 12)}$$

This transfer function is similar to that of a system consisting of a spring of stiffness K in parallel with a damper with damping constant C (Fig. 9):

$$\frac{F(s)}{X(s)} = Cs + K. \qquad \text{(Eq. 13)}$$

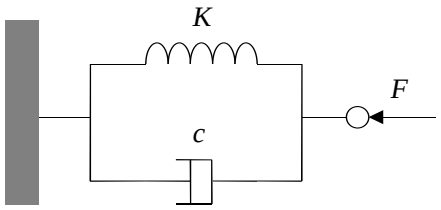

Figure 9. Macroscopic model of cockroach leg used in analysis of sinusoidal displacement response.

In the above model, K and C can be obtained from the

material property parameters *BG'* and *BG''*.

$$K = \frac{BG'}{l^2} \text{ and } C = \frac{BG''}{\omega l^2} \qquad \text{(Eq. 14)}$$

Since *BG'* and *BG''* vary with the vibration frequency, the resulting *K* and *C* are also functions of the frequency. Figure 10 predicts the damping constant according to equation 14. It is shown from the figure that the damping decreases as the vibration frequency increases.

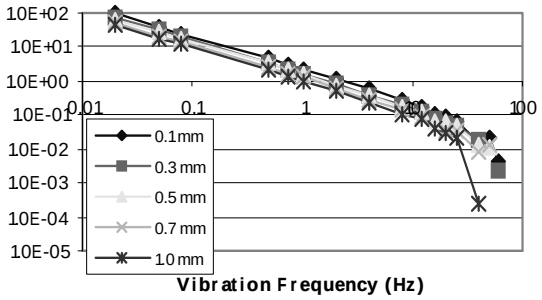

Figure 10. Predicted damping constant as a function of frequency.

The *K* and *C* values obtained from equations 14 can be further used to produce force-displacement hysteresis loops and visually compared with experiment data (Figure 11). The model appears good for low frequencies and small amplitudes of vibration, when the cockroach leg behaves in a linear elastic manner. For frequencies higher than 40 Hz or frequencies higher than 16 to 20 Hz at deflection amplitudes of 0.7 and 1.0 mm, the fit degrades noticeably. This is largely due to the nonlinear nature of the cockroach leg response at these vibration values.

The model can also be evaluated quantitatively. Comparison of the predicted and measured *K* show that they are extremely close; the predictions are lower than measured values by an average of 1%, with a standard deviation of 0.6%.

The energy loss for the viscoelastic material is caused by the internal friction of the material. It is represented by the area within the ellipse of stress vs. strain in dynamic loading. With the stiffness *K* and damping constant *C* obtained before, we are able to calculate the energy dissipation per cycle for different frequencies and compared with the experimental measurement. Figure 12 plots the deviation between predicted and measured energy loss per cycle. The analysis shows that the *C* predictions were more accurate at smaller amplitudes and lower frequencies. For vibration amplitudes of 0.1 mm, 0.3 mm, and 0.5 mm, the average difference was 6% to 10%. For the 0.7 mm and 1.0 mm amplitudes, the difference averaged 30% to 40%.

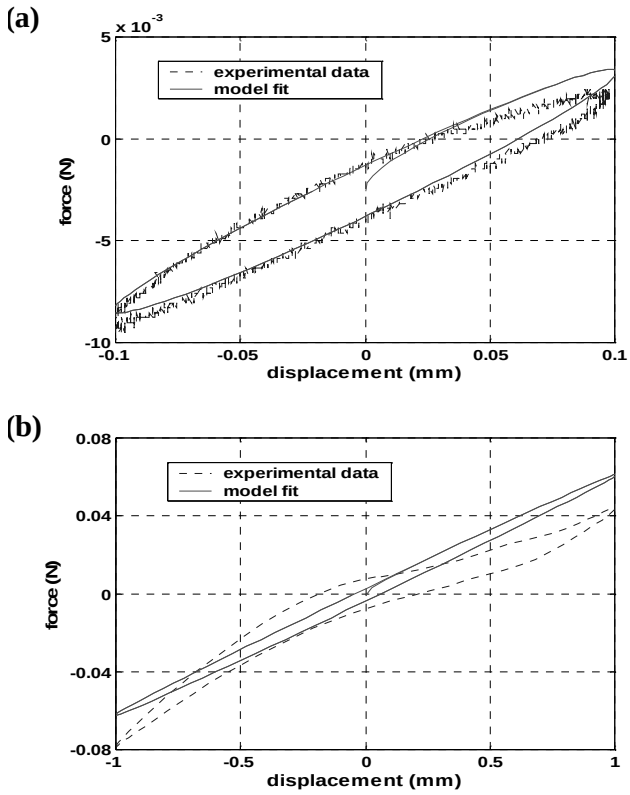

Figure 11. Comparison of Voigt model and experimental data. (a) 0.1 mm and 0.02 Hz, (b) 1.0 mm and 40 Hz.

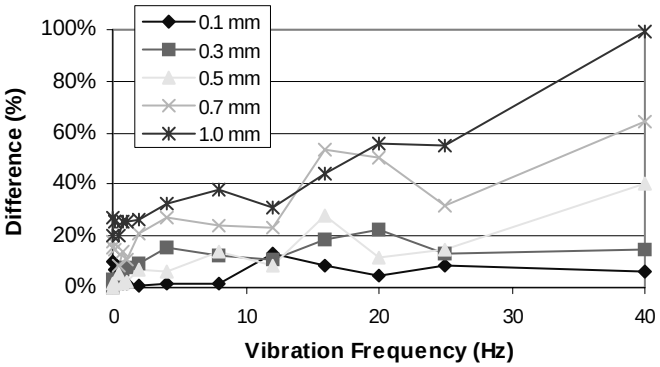

Figure 12. Deviation between predicted (Voigt model) and measured energy loss per cycle.

Evaluation of Model Fit

The lumped-parameter torsional model of the cockroach leg appears to be adequate as an estimation of the behavior of the cockroach leg at the range of amplitudes studied (0.1 mm to 1.0 mm) and at frequencies of less than 40 Hz. For higher frequencies, the cockroach leg deviates significantly from the

linear viscoelastic behavior predicted by these models.

Linkage between relaxation and sinusoidal results

The models shown in Fig. 7 and Fig. 9 are reminiscent of the standard linear solid and the Voigt material models of viscoelastic behavior (Fig. 1). The material properties derived, BG_1, BG_2, BG', and BG'', (the scaled loss modulus, storage modulus, dynamic storage modulus, and dynamic loss modulus, respectively) are also very similar to the *material constants* associated with the standard linear solid model.This motivates us to find a constitutive law for the cockroach leg material that accounts for both the relaxation and sinusoid results.

In linear viscoelastic theory, the Boltzmann superposition integral is used to express dynamic stress history [Lakes, 1999]:

$$\sigma(t) = \int_{-\infty}^{t} E(t-\tau)\frac{d\varepsilon}{d\tau}d\tau = (E' + iE'')\varepsilon(t) \qquad \text{(Eq. 15)}$$

Combining the Boltzmann superposition integral with linear viscoelastic theory enables us to create a link between the constitutive measures G_1 and G_2 and the dynamic measures G' and G''. If the standard linear solid model is used, BG' and BG'', the dynamic storage and loss moduli for sinusoidal shear strain input, can be written in terms of the shear moduli, BG_1 and BG_2: [Lakes, 1999]

$$BG' = BG_2 + \frac{\omega^2\tau^2}{1+\omega^2\tau^2}BG_1 \text{, and } BG'' = \frac{\omega\tau}{1+\omega^2\tau^2}BG_1 \qquad \text{(Eq. 16)}$$

Fig. 13 plots the predicted BG' and BG'' moduli calculated from the values of BG_1 and BG_2. For comparison, BG' and BG'' calculated directly from experimental data (Eq. 10) at an amplitude of 0.3 mm are also plotted.

These plots show that the standard linear solid model is good to build a linkage between BG_1, BG_2, and the dynamic storage modulus BG'. However the dynamic loss modulus BG'' can not be well predicted by a standard linear solid model. This indicates that the properties of viscoelastic material are too complex to be properly modeled by a simple constitutive law. The same observation was reached in other viscoelastic materials [Ferry, 1970] as well as prior experiments with human cortical bone [Lakes, 1979].

The major contradiction between the commonly used linear viscoelastic model and the biological material test for biological materials is that the former predicts a phase shift that decreases to zero as the frequency of excitation decreases. However, this is not true for a cockroach leg excited in a direction orthogonal to joint movement (Fig. 5).

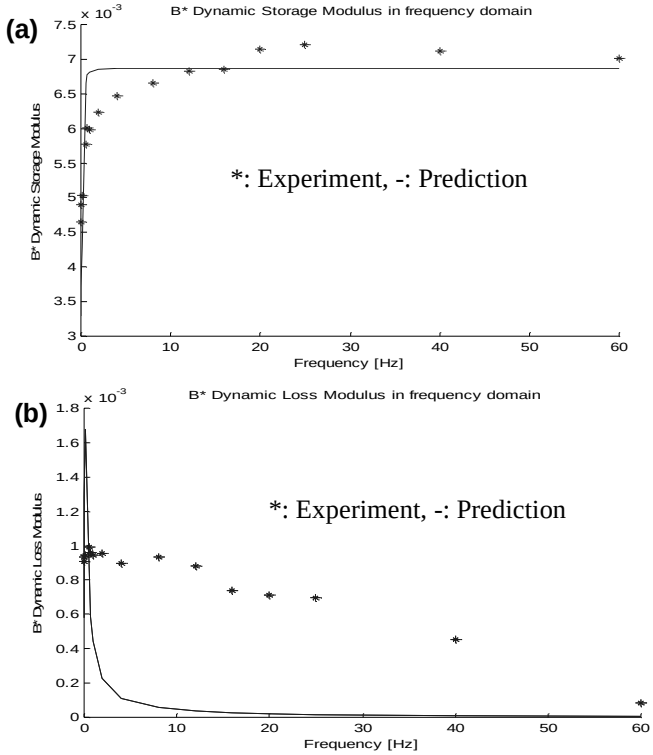

Figure 13. (a) Scaled dynamic storage modulus (BG') calculated from BG_1 and BG_2 and from the experiment, (b) Scaled dynamic loss modulus (BG'') calculated from BG_1 and BG_2 and from the experiment.

The phase shift (or loss angle) is the lag of the strain with respect to stress in a dynamic loading. It is defined as a function of BG' and BG'':

$$\Delta = arc\tan\left(\frac{G''}{G'}\right) = arc\tan\left(\frac{BG''}{BG'}\right) \qquad \text{(Eq. 17)}$$

The phase shift has significant effect on the shape of the hysteresis curve and thus the energy dissipation. In the cockroach leg experiment, the energy dissipation at low frequency is observed to be high, while that for a typical linear viscoelastic model is low. Adaptations of the linear viscoelastic model may yield a better representation of the behavior of materials such as the cockroach leg. With better understanding of how the material characteristics BG_1, BG_2, BG', and BG'' relate to each other, we will better understand and characterize the behavior of biological components such as the cockroach leg.

SDM MATERIAL CHARACTERIZATION

The SDM process offers us the opportunity to integrate a

range of desired impedance into the structure of robot legs for improved robustness and simpler control. SDM-compatible materials span a wide range of material properties and the SDM process enables us to control local variations through Functionally Graded Materials (FGM) [Cham et al, 1999].

An example of a FGM mechanism is shown in Fig. 14. It is a five-bar linkage in which three of the joints have been replaced with flexures. The structural material of the linkage is a grade of polyurethane with high stiffness, while the flexible joint is a soft, viscoelastic polyurethane.

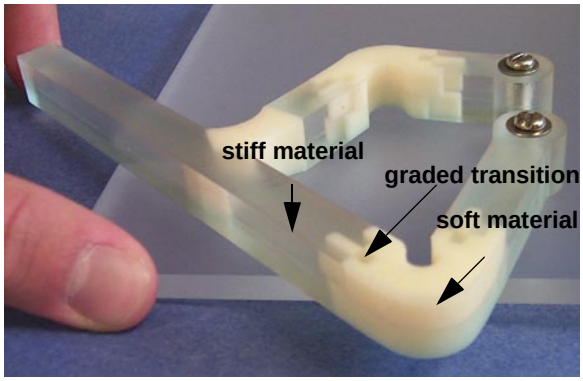

Figure 14. A five-bar linkage with graded materials manufactured by SDM.

To control the compliance and damping associated with mechanisms such as this, material property information beyond what can be obtained from the manufacturer is needed; therefore, these SDM materials must be characterized.

We have developed a dynamic testing machine (Fig. 15) for this purpose. This testing machine is based on a voice coil actuator; the machine controls force input and measures subsequent displacement of the sample. The machine accepts multiple fixtures and can undertake various torsion, bending and tension tests for sample sizes up to 120mm x 120mm x 50mm. The actuator is driven by a current amplifier which outputs the current signal proportional to the output of a signal generator. A 0.9Kg full bridge thin beam load cell with signal conditioning through a strain gauge processor measures the actuating force while a LVDT measures the displacement of the actuator. Data from the load cell and the LVDT are collected via a National Instruments DAQ board controlled by a LabView program.

Dynamic Tests for the SDM Material

The dynamic test was performed on IE 90A polyurethane (Innovative Polymers Inc.) which is used for building soft joints as shown in figure 14. In preparing the sample, the resin and hardener are mixed together by a weight ratio of 38:100. It is then degassed in a vacuum chamber and poured into a wax mold to form a cylindrical sample of 6.35mm in diameter and 63.5mm in length. The demolded sample was aged for 2 more days before the test was performed.The sample was affixed between two coaxial holders, resulting in an effective length of 21.6mm. The upper end of the sample was fixed on the fixture platform, while the lower end was seated in a bearing which can be rotated via an extension arm attached to the voice coil actuator. The link mechanism between the actuator and the sample clamp was designed for minimum friction. The sinusoidal force was generated and the actuator displacement was recorded for a vibration frequency ranging from 0.2Hz to 20Hz. Figures 15 and 16 show the resulting loss angle, dynamic loss modulus and storage modulus following a similar procedure to that in the cockroach leg analysis.

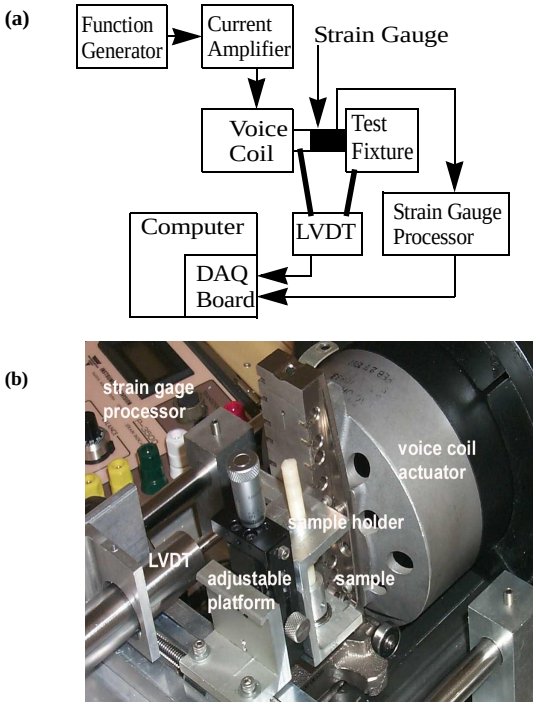

Figure 15. (a) Schematic drawing of test machine. (b) Close view of the test machine

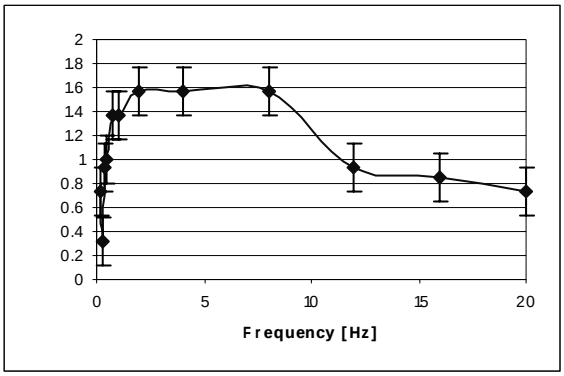

Figure 16. Loss angle in a frequency range from 0.2Hz to 20Hz for soft polyurethane material.

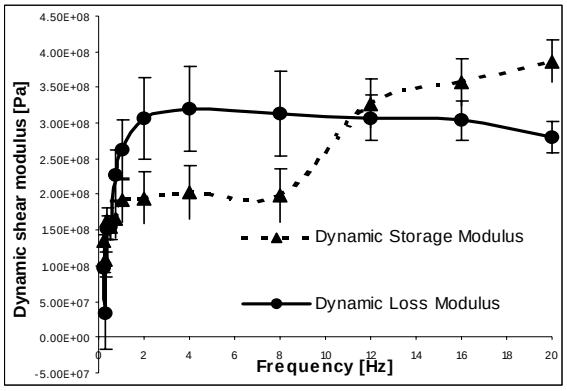

Figure 16. Dynamic storage *G'* and loss *G"* moduli for the soft polymer material.

The possible error sources in the test are listed below:

1. - inertia and the friction of the clamp and the extension arm that move with the bottom end of the sample.The effect of inertia is shown in Eq. 6. The inertia and the friction of the sample cause at most 0.2N or 10% error on the force measurement at the 20Hz frequency.
2. - aging of the material which leads to the variation in viscoelastic property. The material tends to become harder after days of aging.
3. - accuracy of the load cell. The load cell we are using has a 0.9Kg full scale range and can reach an error level of +-20mN or +-1%.The error level can be reduced by calibrating the sensor, using smaller range sensors and increasing the displacement range of the test.

Design of Biomimetic Legs

With information regarding the mechanical behavior of animal legs and the material behavior of SDM materials, we are able to develop guidelines for biomimetic leg design. Previous research has demonstrated that most animals can be modelled as bouncing, spring-mass monopodes despite impressive variations in leg number, leg length, position, and exoskeleton/ endoskeleton. This is because the energetics and dynamics of trotting, running, and hopping animals are dynamically similar within the locomotion method [Blickhan and Full, 1993] [Blickhan, 1989].

For animals to locomote in a dynamically similar manner, the relative vertical stiffness (K_{rel}) expressed in Eq. 18 must be relatively constant across animals utilizing the same type of locomotion method.

$$K_{rel} = \frac{F}{(mg)} \Big/ \frac{\Delta L}{L} \qquad \text{(Eq. 18)}$$

Where L is a characteristic leg length determined by the leg length, the locomotion scheme, and the number of legs of the animal, F_v is the vertical force applied by the animal on the ground during midstance, and ΔL is the change in leg length that results from this vertical force. For trotters, the relative whole body stiffness K_{rel} ranges from 7.1 (turkey) to 25.6 (kangaroo rat) but averages around 18.6[Blickhan and Full 1993].

The whole vertical body stiffness at midstance for a specific animal is:

$$K = \frac{F}{\Delta L} = \frac{K_{rel}}{L} \qquad \text{(Eq. 19)}$$

According to the viscoelastic model discussed previously, this leg stiffness can be expressed as a function of the complex dynamic modulus and the leg geometry:

$$K_{leg} = \frac{B|G^*|}{L^2} \qquad \text{(Eq. 20)}$$

Where B is a geometric factor, L is the characteristic leg length, and $|G^*|$ is the magnitude of the dynamic modulus that varies with respect to the vibration frequency.

Insects tend to run at their natural frequencies to maximize energy economy [Blickhan 1989]. This frequency can be estimated from the vertical stiffness obtained from the monopode model.

$$f = \frac{1}{2\pi}\sqrt{\frac{K}{m}} \qquad \text{(Eq. 21)}$$

Eq. 18 through Eq. 21 build a set of guidelines for relating animal size, characteristic leg length, leg stiffness, locomotion frequency, and leg material property for animals using similar locomotion methods. Let us consider these guidelines with respect to Nature's design on the cockroach leg. A *Blaberus discoidalis* is a trotter with body mass of approximately 0.003 kg. Geometric scaling against other trotters yields a virtual leg length of 0.02 m. These values enable us to estimate the vertical whole body stiffness as 25 N/m and the natural frequency as 91 rad/sec (14 Hz). At this frequency, the linear viscoelastic model predicts a magnitude of $B|G^*|$ of 0.0069 Nm. Plugging this value into Eq. 20 yields a leg stiffness of 18 N/m.

For comparison, data from the cockroach used to form the monopode model yields an estimated vertical whole body stiffness closer to 32 N/m. If we assume that the vertical whole body stiffness of the *Blaberus* is evenly distributed among the three legs of a tripod, then the individual leg stiffness should be approximately 11 N/m. These observed and measured leg stiffnesses are similar. The differences largely result from approximations made in the monopode model and the dynamic modulus being obtained in a direction not exactly vertical to the ground at midstance.

Having reviewed these equations for the cockroach leg, let us attempt the design of a biomimetic leg. For a trotting robot with a target mass of 0.26 kg and a characteristic leg length of 100 mm, the monopode model predicts the total vertical body stiffness as 430 N/m. If this robot is a hexapod walking machine with a tripod gait, the average stiffness per leg is approximately 140 N/m.

The simplest case of leg design might be a soft polyurethane rod with diameter D and length L_{joint} connected to a stiff linkage of length L. Then L_{joint} is:

$$L_{joint} = \frac{\pi D^4 \cdot |G^*|}{32 L^2 \cdot K_{leg}} \qquad \text{(Eq. 22)}$$

Where $|G^*|$ is the magnitude of the dynamic modulus.

In order to find |G*|, we must first estimate the locomotion frequency. The monopode model sets this at 6.5 Hz. The $|G^*|$ value for the soft polyurethane material we have characterized is about 4 x 10^8 Pa at that frequency range. If we make the diameter of the rod 3.2mm, the required joint length L_{joint} is 4.8mm.

The above example is only an exercise demonstrating the simplest case of the leg design. The leg is biomimetic only with respect to stiffness and damping, but not in other aspects of function. Real biomimetic legs are more complex due to different loading conditions and joint geometry. However, once the dynamic modulus property of the joint material is obtained, one can always design the joint structure for the target leg stiffness.

CONCLUSIONS

Some polymer materials that can be used in SDM are similar to the biological materials found in insect legs that exhibit viscoelasticity. This inspires us to develop material models and design methodologies that can be used to guide biomimetic robot leg design and material selection. In this paper, we have discussed a simple lumped parameter model used to characterize cockroach leg behavior in relaxation experiments and a linear model for characterizing leg response to sinusoidal excitations. We have also developed a dynamic test machine and characterized a polyurethane material used for SDM fabrication of robot joints.

The current model assumes linear viscoelasticity. The correlation between the models and the results of experiments is relatively good at low frequencies and small displacements but deteriorates at higher frequencies and displacements as nonlinear effects become pronounced. At very low frequencies dynamic tests on cockroach legs indicate a higher loss modulus than that predicted by a standard linear model. This inspires us to develop a new material constitutive law to better simulate the viscoelastic behavior of the leg in a wide frequency range.

The effects of inertia and strain hardening effect have also been neglected for making biomimetic robot limbs using SDM. Further work will include more realistic models and the development of design rules.

ACKNOWLEDGMENTS

The authors thank the members of the Stanford DML and RPL teams for their contributions to the work documented in this paper. Special thanks also to the members of the Berkeley PolyPEDAL Lab for their open communication and technical contributions to this work. Wendy Cheng is supported by a combined NSF and Stanford Graduate Fellowship. This work is supported by the National Science Foundation under grant MIP9617994 and by the Office of Naval Research under N00014-98-1-0699.

REFERENCES

Alexander, R. M., 1990, “3 uses for springs in legged locomotion,” *International Journal of Robotics Research, Vol. 9 (#2),* pp. 53-61.

Bailey, S. A.; Cham, J. G.; Cutkosky, M. R.; Full, R.J., 1999, “Biomimetic robotics mechanisms via shape deposition manufacturing,”

Binnard, M., 1999, “Design by composition for rapid prototyping,” Ph.D. Dissertation, Stanford University, Stanford, CA.

Blickhan, R., 1989, “The spring-mass model for running and hopping,” *Journal of Biomechanics, Vol. 22 (#11-1),* pp. 1217-1227.

Blickhan, R., 1986, “Stiffness of an arthropod leg joint,” *Journal of Biomechanics, Vol. 9 (#5),* pp. 375-384.

Blickhan, R. and Full, R.J., 1993, “Similarity in multilegged locomotion: bouncing like a monopode”, *Journal of Comparative Physiology A, Vol. 173 (#5),* pp. 509-517.

Cavagna, G.A.; Mantovani, M.; Willems, P.A.; Musch, G., 1997, “The resonant step frequency in human running,” *Pflugers Archive - European journal of Physiology, Vol. 434 (#6),* pp.678-684.

Cham, J.G.; Pruitt, B.L.; Cutkosky, M.R.; Binnard, M.; Weiss, L.E.; Neplotnik, G., 1999, “Layered manufacturing with embedded components: process planning issues,” *ASME Proceedings, DETC '99.* Las Vegas, Nevada. September 12-15.

Eagner, H. and Blickhan, R., 1999, “Stabilizing function of skeletal muscles: an analytic investigation.” *Journal of Theoretical Biology, Vol. 19,* pp. 163-179.

Brown, I.E. and Loeb, G.E. “A reductionist approach to creating and using neuromusculoskeletal models,” In *Biomechanics an dNeural Control of Posture and Movement* (Eds. Winters, J.M. and Crago, P.E.), In Press.

Farley, C.T.; Glasheen J.; McMahon, T.A., 1993, “Running springs: speed and animal size,” *Journal of Experimental Biology, Vol. 185,* pp. 71-86.

Farley, C.T. and Gonzales, O., 1996, “Leg stiffness and stride frequency in human running,” *Journal of Biomechanics, Vol. 29 (#2),* pp. 181-186.

Farley, C.T.; Houdjk, H.H.P., Vanstrien, C., and Louie, M., 1998, “Mechanism of leg stiffness adjustment for hopping on surfaces of different stiffness,” *Journal of Applied Physiology, Vol. 85 (#3),* pp. 1044-1055.

Ferris, D.P. and Farley, C.R., 1997, “Interaction of leg stiffness and surface stiffness during human hopping,” *Journal of applied Physiology, Vol. (82),* pp. 15-22.

Ferris D.P.; Liang, K.L.; Farley, C.R., 1999, “Runners adjust leg stiffness for their first step on a new running surface,” *Journal of Biomechanics, Vol. 32 (#8),* pp. 787-794.

Ferris D.P.; Louie M.; Farley C.R., 1998, “Running in the real-world: adjusting leg stiffness for different surfaces,” *Proceeding of the Royal Society of London Series B - Biological Sciences, Vol. 265 (#1400),* pp. 989-994.

Ferry, J.D., *Viscoelastic Properties of Polymers,* 1970, John Wiley & Sons, New York.

Fessler J.; Nickel, A.; Link, G.; Prinz, F.; Fussel, P., 1997, “Functional gradient metallic prototypes through shape deposition manufacturing,” *Proceedings of the Solid Freeform Fabrication Symposium*, Austin, TZ, September, 1997, pp. 521-528

Full, R.J., 1993, “Integration of individual leg dynamics with whole body movement in arthropod locomotion,” in *Biological Neural Networks in Invertebrate Neuroethnology and Robots.* (eds. R. Beer, R. Ritzmann and T. McKenna). Academic Press. Boston. pp. 3-20.

Full, R.J. and Koditschek, D. E., 1999, “Templates and Anchors - Neuromechanical hypotheses of legged locomotion on land,” *Journal of Experimental Biology, Vol. 202,* pp. 3325-3332.

Full, R.J. and Tu, M.S., 1990, “The mechanics of 6-legged runners,” *Journal of Experimental Biology, Vol. 148,* pp. 129-146.

Fung, Y.C., 1994, “Chapter 7: Biovisceoelastic Solid” in *Biomechanics: Mechanical Properties of Living Tissues.*

Kubow, T.M. and Full, R.J., 1999, “The role of the mechanical system in control: a hypothesis of self-stabilization in hexapedal runners,” *Philosophical Transactions of the Royal Society of London B, Vol. 354,* pp. 849-862.

Lakes, R.S.; 1999. *Viscoelastic Solids*, CRC press, Boca Raton.

Lakes, R. S.; Katz, J. L.; Sternsterin, S.S., 1979a, “Viscoelastic properties of wet cortical bone 1: torsional and biaxial studies,” *Journal of Biomechanics, Vol. 12 (#9),* pp. 657-678.

Lakes, R. S.; Katz, J. L.; Sternsterin, S.S., 1979b, “Viscoelastic properties of wet cortical bone 1: relaxation mechanisms,” *Journal of Biomechanics, Vol. 12 (#9),* pp. 679-687.

Meijer, K. and Full, R. J., “Stabilizing properties of invertebrate skeletal muscle.” American Zoologist. In press.

Merz, R.; Prinz, F.B.; Ramaswami, K.; Terk, M.; Weiss, L., 1994, “Shape deposition manufacturing,” *Proceedings of the Solid Freeform Fabrication Symposium.* University of Texas at Austin, August 8-10.

: Obusek, J ; Holt, K ; Rosenstein, R , “The hybrid mass-spring pendulum model of human leg swinging: stiffness in the control of cycle period”, *Biological cybernetics*, Vol 73, pp. 139 1995

Raibert, M.H., 1986, *Legged Robots that Balance*, MIT Press, CAmbridge, MA.

Suresh, S. and Mortenen, A., 1998. *Fundamentals of functionally graded materials*, IOM Communications Ltd, London, U.K.

Viale, F.; Dalleau, G.; Greychat, P.; Lacour, J. R., and Belli, A., 1998, “Leg stiffness and foot orientations during running,” *Foot & Ankle International, Vol. 19 (#11),* pp. 761-765.

Vogel, S., “Better Bent Than Broken”, *Discover*, vol. 16, No. 5, pp 62, 1995